

# A Study on the Distortion Caused by Spot Heating with Air Cooling

S. B. Shin and J. G. Youn

## Abstract

This paper deals with the optimum condition for spot heating to correct the thin buckled panel caused by welding. Heat input models for each flame torch tip (500, 800, 2000) with standoff were established using FEA to evaluate the temperature distribution of the heated plate and verified by experiment. With the heat input models developed for each torch tip, the effect of heating variables including ramp ratio(R) and standoff on the radial shrinkage and angular distortion was identified using FEA. Based on the results, the proper conditions of spot heating with air cooling were established. The amount and distribution of the radial shrinkage by spot heating were formulated as the function of heating variables and in-plane rigidity of the plate.

**Key Words :** Spot heating, Finite element analysis(FEA), Heat input model, Ramp ratio, Standoff, Radial shrinkage.

## 1. Introduction

Panels are fundamental components in a welded steel structure, which are strengthened by welding longitudinal and transverse stiffeners. Typically, panels are constructed by a series of welding procedures: 1) butt welding of individual plates to form the blanket 2) mechanical fillet welding to attach longitudinal stiffeners to the blanket 3) manual welding of transverse stiffeners to form grid structure. For structural effectiveness, the plate thickness of a deck structure has been gradually reduced in order to reduce self-weight and maintain a low overall center of gravity of the structure. When the thin plates are welded, residual compressive stress is developed in certain area away from the weld and cause "oscillations" in the steel plate located between stiffeners and along plate edges. That is, the buckling distortion occurs when the shrinkage force caused by welding exceeds the buckling strength of the welded

structure. The best way to control the buckling distortion is to optimize the structural parameters and welding parameters including plate thickness, stiffener spacing, heat input, the accuracy of fit-up and so on. However, the problems related to the buckling distortion of the thin welded structure such as deck structure have been reported continuously. Costly correction work of the buckling distortion is then followed. A general correction method is to heat the plate either at selected spots or along certain lines and then to cool it. The heating procedure is generally established by experiences, not by engineering approach. Although several papers have been written on flame heating, scientific data is not sufficient.

This study has tried to establish the proper conditions of spot heating with air cooling to correct the buckled panel using a finite element analysis (FEA). In order to do it, heat input models for each flame torch tip (500, 800, 2000) with standoff (h) were established to evaluate the temperature distribution of the heated plate and verified by experiment. With the heat input models established for each tip, the effect of heating variables including ramp ratio(R) and standoff (h) on the radial shrinkage and angular distortion was identified using FEA. Based on the results, the proper

---

*S. B. Shin* and *J. G. Youn* : Hyundai Industrial Research Institute, Hyundai Heavy Industries Co. Ltd, Ulsan, Korea  
E-mail : str@hhi.co.kr

conditions of spot heating using air cooling were established. The amount and distribution of the radial shrinkage by spot heating were formulated as function of heating variables and in-plane rigidity of the plate.

## 2. Heat input model

### 2.1 Experiment and analysis procedure

The temperature distribution of the spot heated plate is very important to calculate the amount and distribution of a radial shrinkage generated by a spot heating. The temperature distribution at the heated plate depends on the amount of thermal energy generated by the chemical reaction of oxygen and fuel gas. That is, the characteristics of the flame, which are the efficiency and distribution of heat flux, must be identified with heating variables such as the oxygen to fuel gas ratio, tip number, standoff (h) and so on. However, it is difficult to evaluate the characteristics of flame using analytical solution and CFD (Computerized Fluent Dynamics).<sup>1)</sup> In This study, the characteristic values of the flame were determined by comparing the temperature distribution obtained by experiment with that from FEA. The change and distribution of temperature at the each point of the heated plate during heating and cooling time were measured with K type thermocouple (under 2.3mm from the heated surface) and data logging system (see Fig. 1).

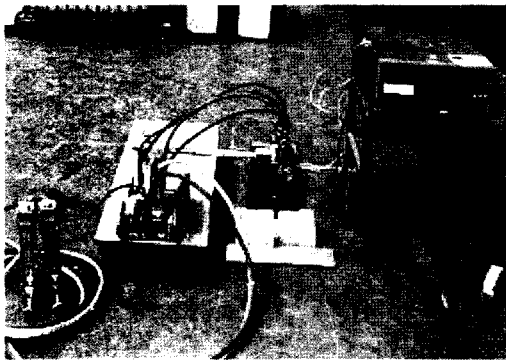


Fig.1 Experiment for temperature measurement

Table 1 and Fig. 2 show the schematic diagram of the heated plate and heating variables used for experiment and FEA. The flame torch tips used for the experiment are typical torch tips for heating and the plate used was A-grade steel for shipbuilding. The flow rate of fuel gas and the travel speed of heating torch were controlled at a constant value. Based on the experimental results, the efficiency of thermal energy and the distribution of heat flux of the gas flame were identified by finite element analysis (FEA).

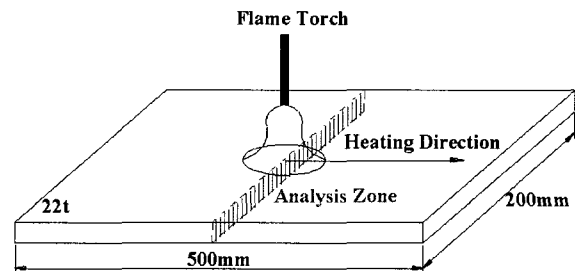


Fig. 2 Schematic diagram of model used for experiment and FE analysis

Table 1 Variables used for experiment

t [mm]	Tip No.	Flow rate [L/min]		Standoff [mm]	Heating speed [mm/min]
		O <sub>2</sub>	LNG		
22	500	20	15	20 - 100	150
	800				
	2000				

Heat input models for each torch tip (500, 800 and 2000) used for FEA were specified by a double Gaussian mode of heat flux with the 1st and the 2nd flame as shown in equation (1).<sup>2)</sup>

$$q(r) = \frac{6\eta Q}{\pi(R_1^2 + \beta R_2^2)} \left( e^{-\frac{6r^2}{R_1^2}} + \beta e^{-\frac{6r^2}{R_2^2}} \right) \quad (1)$$

$q(r)$  is the amounts of heat flux along the distance from flame torch center,  $Q$  is the total thermal energy generated by chemical reaction of oxygen and LNG,  $\eta$  is the efficiency of thermal energy,  $R_1$  and  $R_2$  are the length of the 1st and the 2nd flame respectively,  $\beta$  is characteristic coefficient of the 2nd flame.

For heat transfer analysis, 3 dimensional characters of the heat transfer problem can be simplified to two dimensional problem with the assumption that the flame heat source is moving at a constant speed along a regular path, and the heating speed is sufficiently high relative to the material's characteristic diffusion rate and end effects resulting from either initiation or termination of the heat source can be neglected. This can be achieved by analyzing a cross-section of the plate of unit thickness and located in the mid-length region of the weld (see Fig. 2). Table 2 shows the variables used for the heat transfer analysis. Based on the parametric FE analysis, the efficiency of thermal energy, the flame length and  $\beta$  were determined.

Table 2 Variables used for FEA

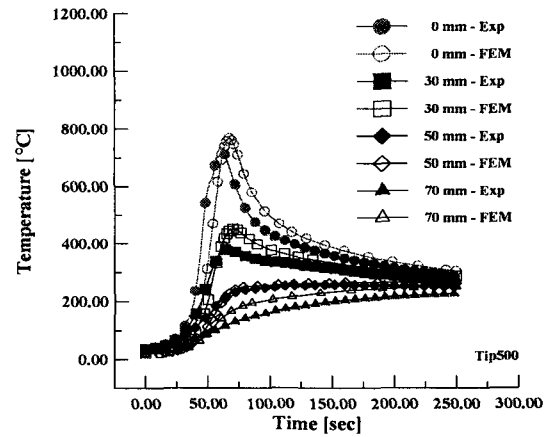
t [mm]	Efficiency	Standoff [mm]	Flame		
			$R_1$	$R_2$	$\beta$
22	0.3 - 0.7	20 - 100	30 - 100	100 - 200	0.1 - 0.5

### 2.2 Experimental and analysis results

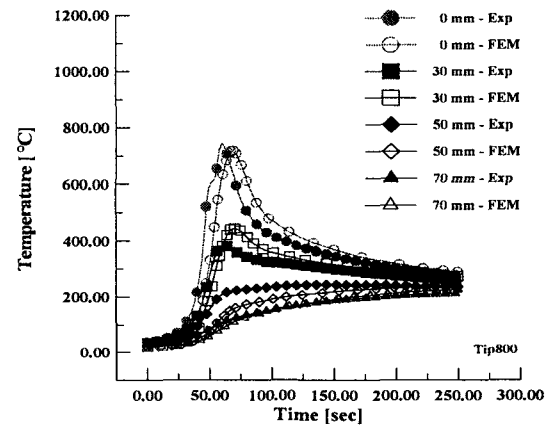
Fig. 3 shows the changes of temperature at the each point of the heated plate with tip obtained by FEA and experiment with time for each tip (see Fig. 2.). The standoff (h) was 20mm. As shown in Fig. 3, the results of FEA and experiment are coincident each other comparatively. This indicates that the characteristics of the flame, which are efficiency of thermal energy and the effective radius of the flame determined by parametric FEA, are valid.

Fig. 4 shows the efficiency of thermal energy and effective radius of heat flux for each tip. effective radius of flame is  $R_1 + \beta R_2$ . As shown in Fig. 4, the efficiency of thermal energy of torch tip number 800 is better than that of the others selected in this study. In addition, the effective radius of heat flux of tip number 800 is smaller than that of the others. These results indicate that torch tip number 800 is adequate to correct the buckled plated by spot heating. It is because the temperature gradient along the thickness direction decreases almost in a linear manner with a decrease in

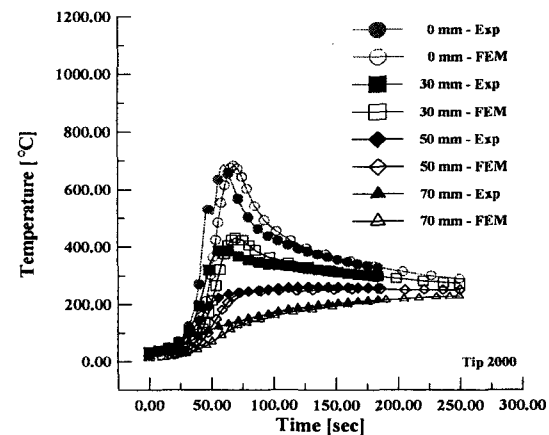
the effective radius of flame.



(a) Torch tip 500



(b) Torch tip 800



(c) Torch tip 2000

Fig. 3 Changes of temperature at the each measuring point of the heated plate with time for each torch tip

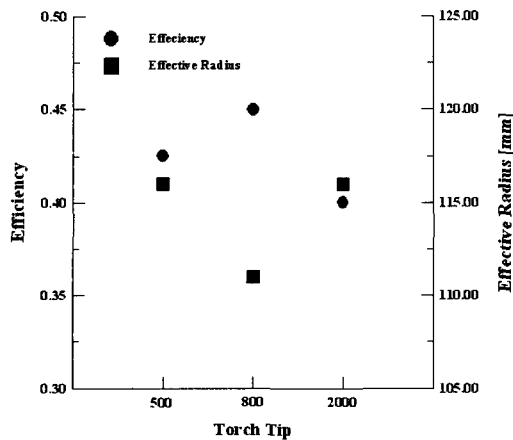


Fig. 4 Efficiency of the thermal energy and effective radius of heat flux of flame for each torch tip

Fig. 5 shows the variation of the efficiency of thermal energy  $e$  and the effective radius of heat flux of flame with standoff ( $h$ ) of torch tip number 800. As shown in Fig. 5, the efficiency of thermal energy and effective radius of heat flux decrease with an increase of standoff. This tendency results from the fact that the heat transfer mechanism between the flame and the plate is governed by convection and radiation.

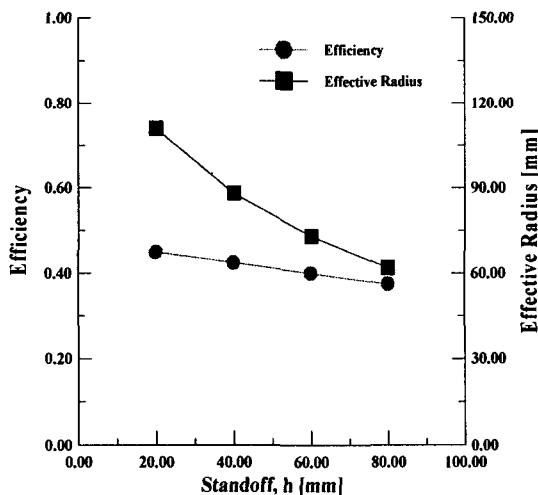


Fig. 5 Variation of the efficiency of the thermal energy and the effective radius of heat flux of flame with standoff of torch tip 800

### 3. Optimum heating condition

To correct the buckled thin plate caused by welding process, the conditions of spot heating must be established which can maximize the amount of the radial shrinkage and minimize the amount of the angular distortion at the same time. In order to do it, the effect of spot heating variables including tip number (2000 and 800), standoff (20-80mm) of torch tip and ramp ratio (0.1 - 1.0) on the radial shrinkage and angular distortion was investigated by thermo-mechanical analysis with heat input model established in this study. Ramp ratio ( $R$ ) is a ratio of holding time to total heating time as shown in Fig. 6. Mesh design used for the thermo-mechanical stress analysis consisted of 8-nodes plane element. Mechanical properties of the heated area were postulated to behave as an isotropic, elasto-plastic and strain-hardening continuum. Yielding of material was assumed to be governed by von-Mises criteria.

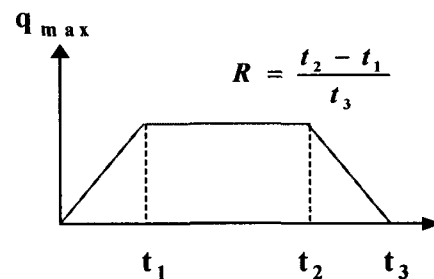
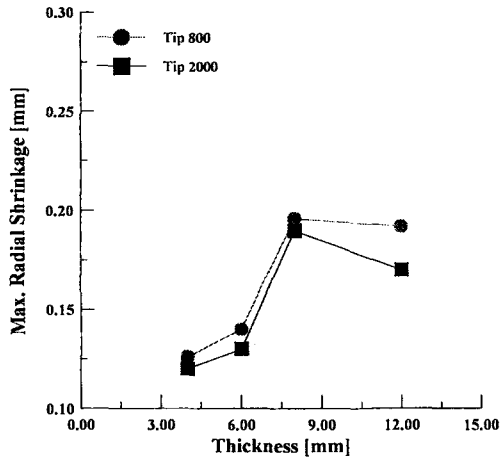


Fig. 6 Ramp ratio of spot heating

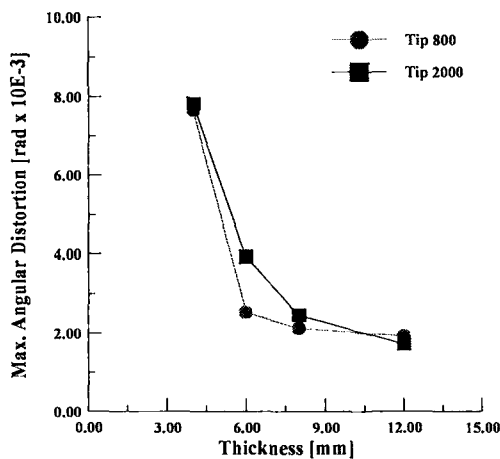
#### (1) Torch Tip

Variation of the maximum radial shrinkage and angular distortion by spot heating with plate thickness (4.5 - 12mm) for each torch tip is shown in Fig. 7. Table 3 represents the spot heating conditions used for FEA. As shown in Fig. 7 (a), the maximum radial shrinkage at the heated plate obtained by torch tip 800 is larger than that by torch tip 2000 regardless of the plate thickness. In addition, the angular distortion at the plate heated with torch tip 800 is generally small compared with torch tip 2000. This tendency increases with an increase in the plate thickness. These results verify that the torch tip 800 is more suitable than torch tip number in terms of the correction effect of the buckled thin plate. This tendency increases with an increase in the plate thickness. These results verify that

the torch tip 800 is more suitable than torch tip number in terms of the correction effect of the buckled thin plate.



(a) Maximum radial shrinkage



(b) Maximum angular distortion

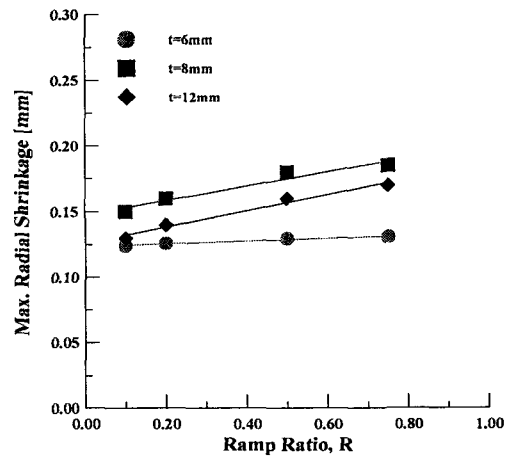
Fig. 7 Variation of the maximum radial shrinkage and the maximum angular distortion by spot heating with plate thickness for each torch tip by FEA

Table 3 Spot heating conditions used for FEA related to Fig. 7

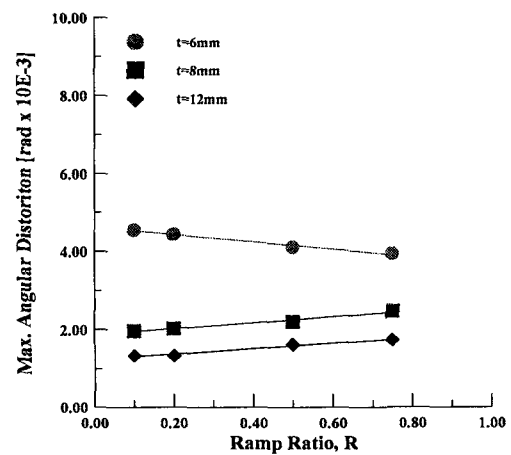
t [mm]	Heating time [sec]	Flow rate [L/min]		Standoff [mm]	Ramp ratio
		O <sub>2</sub>	LNG		
4.5 - 12	9.0 - 24.0	20	15	20	0.7

(2) Ramp ratio (R)

Fig. 8 (a) and (b) show the variation of the maximum radial shrinkage and angular distortion at the plate with ramp ratio(R) and plate thickness by FEA respectively. The spot heating conditions used for FEA are given in Table 4. When the plate thickness is above 8mm, the maximum radial shrinkage by spot heating increases with an increase in ramp ratio, and the angular distortion slightly increases with an increase in ramp ratio (R). However, when the plate thickness is 6mm, the radial shrinkage is almost constant regardless of a ramp ratio(R) but the angular distortion decreases with an increase in ramp ratio.



(a) Maximum radial shrinkage



(b) Maximum angular distortion

Fig. 8 Variation of the maximum radial shrinkage and the maximum angular distortion at the plate with ramp ratio and plate thickness by FEA

Table 4 Spot heating conditions used for FEA related to Fig. 8

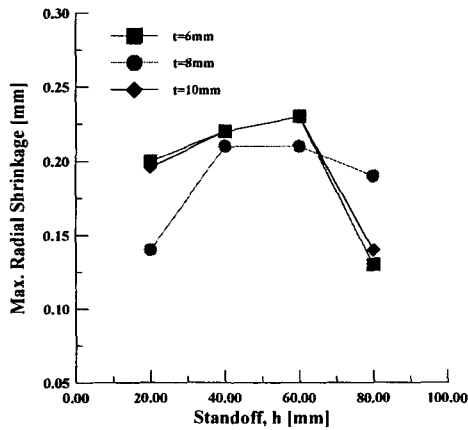
t [mm]	Heating time [sec]	Flow rate [L/min]		Standoff [mm]
		O <sub>2</sub>	LNG	
6 -12	12.0 -24.0	20	15	60

Table 5 Spot heating conditions used for FEA related to Fig. 9

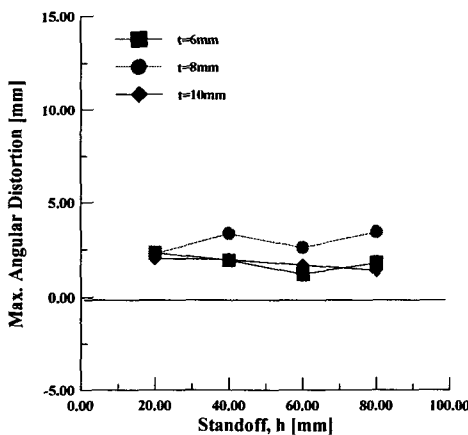
t [mm]	Heating time [sec]	Flow rate [L/min]		Ramp Ratio
		O <sub>2</sub>	LNG	
6 -10	12.0 -20.0	20	15	0.7

(3) Standoff (h)

Fig. 9 (a) and (b) show variation of the maximum radial shrinkage and angular distortion by spot heating by FEA with standoff(h), which is the distance between the end of torch tip and surface of the heated plate. The spot heating conditions used for FEA are shown in Table 5.



(a) Maximum radial shrinkage



(b) Maximum angular distortion

Fig. 9 Variation of the maximum radial shrinkage and angular distortion at the spot heated plate with standoff of torch tip by FEA

As shown in Fig. 9 (a), the maximum radial shrinkage by spot heating linearly increases up to standoff (h) of 60mm and then decreases sharply. The maximum angular distortion under the heating conditions of Table 5 is constant as shown in Fig. 9 (b). From the FEA results obtained with respect to torch tip, ramp ratio (R) and standoff (h), the proper spot heating conditions to correct the buckled thin plate caused by welding process are established as shown in Table 6.

Table 6 Proper spot heating condition to correct the buckled plate established by this study

Torch tip	Ramp ratio, R	Standoff, h [mm]
800	1.0	40 - 60

### 4. Formulation of radial shrinkage

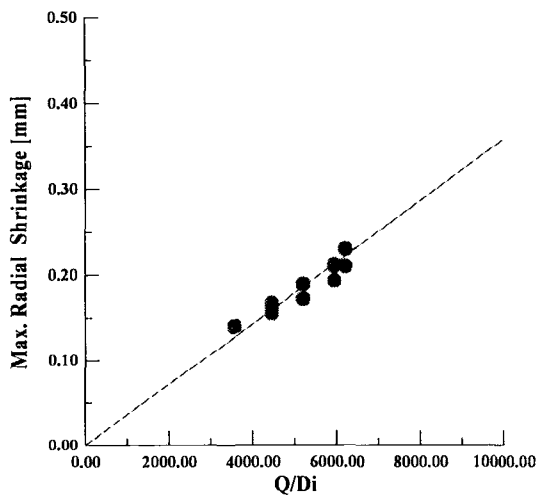
In order to design the automatic correction system for the buckled thin panel structure using spot heating, the amount and distribution of the radial shrinkage should be formulated quantitatively. It is because the deformed shapes at each location of the buckled plate after each spot heating should be predicted to determine the location of the additional spot heating. the radial shrinkage by the spot heating condition established by this study was evaluated by FEA and the distribution of the radial shrinkage was investigated by analytical solution.

#### 4.1 Amounts of radial shrinkage

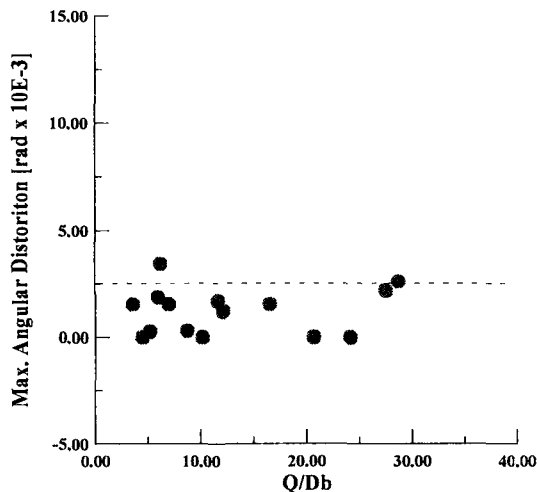
Fig. 10 (a) and (b) show the variation of the

maximum radial shrinkage and the maximum angular distortion as a ratio of thermal energy ( $Q$ ) to in-plane or bending rigidity of the plate ( $D_i$  and  $D_b$ ). As shown in Fig. 10 (a), the maximum radial shrinkage linearly increases with an increase in the ratio of thermal energy ( $Q$ ) to in-plane rigidity ( $D_i$ ) and can be defined as equation (2). However, the angular distortion is nearly constant and below " $2.5 \times 10^{-3}$  radian", regardless of the ratio of the effective thermal energy ( $Q$ ) to bending rigidity ( $D_b$ ) of the plate, as shown in Fig. 10 (b).

$$u_{\max} = f\left(\frac{Q}{D_i}\right) \tag{2}$$



(a) Maximum radial shrinkage



(b) Maximum angular distortion

Fig. 10 Variation of the maximum radial shrinkage and angular distortion by spot heating with  $f(Q/D_i)$  and  $f(Q/D_b)$

### 4.2 Distribution of the radial shrinkage

The radial shrinkage at each location of the spot heated plate depend on the distance from the center of heating torch due to the internal restraint of the plate. In this study, the analytical approach was employed to define the radial shrinkage distribution by spot heating. To do it, an infinite thin plate spot heated by spot heating was assumed to be a large thin plate having a circular hole subjected to uniform external compressive pressure ( $P_e$ ) in the radial direction as shown in Fig. 11.  $r_i$  is the distance from the center of the flame to the location subjected to a half of the maximum heat flux, which is determined by combining equation (1) and Fig. 4.

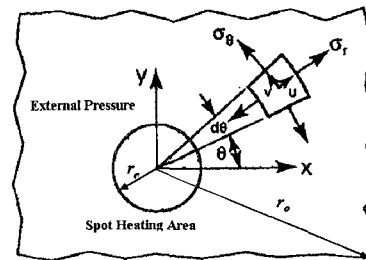


Fig. 11 A large thin plate with a small circular hole

Fig. 11 shows a large thin plate having a small circular hole subjected to uniform pressure. Since the axial load is absent,  $\sigma_z$  is zero. The stresses and deformation are clearly symmetrical with respect to the  $z$ -axis. The symmetry argument also indicates that the shear stress must be zero. Therefore, The polar equations of equilibrium of the system given in Fig. 11 is

$$\frac{d\sigma_r}{dr} + \frac{\sigma_r - \sigma_\theta}{r} = 0 \tag{3}$$

$\sigma_r$  and  $\sigma_\theta$  denote the radial and tangential stresses acting normal to the sides the element. Consider now the radial and tangential displacement  $u$  and  $v$ , respectively. There can be no tangential displacement in the symmetrical field; that is,  $v = 0$ . A point represented by the element in the figure will thus radially as a consequence of loading, but not

tangentially. On the basis of displacements indicated, the strains become

$$\epsilon_r = \frac{du}{dr}, \quad \epsilon_\theta = \frac{u}{r}, \quad \gamma_{r\theta} = 0 \quad (4)$$

Substituting  $u = r\epsilon_\theta$  into the first equation in equation (4), a simple compatibility equation is obtained :

$$r \frac{d\epsilon_\theta}{dr} + \epsilon_\theta - \epsilon_r = 0 \quad (5)$$

The unique solution for the radial shrinkage distribution ( $u(r)$ ) can be determined by the equations of equilibrium, the strain displacement compatibility and Hooke's law as follow.

$$u(r) = A \frac{r_i^2 P_e}{r_o^2 - r_i^2} + B \frac{r_o^2 r_i^2 P_e}{(r_o^2 - r_i^2) r} \quad (6)$$

A and B are

$$A = \frac{1-\nu}{E}, \quad B = \frac{1+\nu}{E} \quad (7)$$

the external pressure ( $P_e$ ) subjected to the  $r_i$  of the spot heated plate is determined by combining equation (2) and (6) :

$$P_i = \frac{u_{max}}{\frac{Ar_o^2 - Br_i r_o^2}{r_o^2 - r_i^2}} \quad (8)$$

### 4.3 Validation of predictive equation for radial shrinkage

FE analysis was performed to verify the predictive equation for the radial shrinkage distribution by spot heating established using analytical solution. The plate used for FEA is 1000(L)x1000(W)mm, external pressure ( $P_e$ ) is -1.0kgf/mm<sup>2</sup>,  $r_i$  and  $r_o$  are 25, 500mm respectively. Fig. 12 compares the results of the radial shrinkage distribution obtained by FEA and equation (6). As shown in Fig. 12, the radial shrinkage at the plate decreases with an increase in the distance from the torch center. Good agreement between the results by two methods can be found.

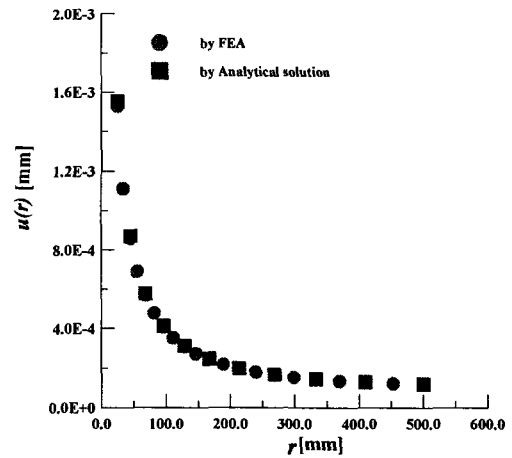


Fig. 12 Results of the radial shrinkage at the plate subjected to the unit pressure by both analytical solution and FEA

Fig. 13 shows the comparison results of radial shrinkage by spot heating with heating time using predictive equation and experiment. The plate thickness was 4.0 mm and the proper spot heating conditions of Table 6 were used. As shown in Fig. 13, the amount and distribution of radial shrinkage obtained by the predictive equation are coincident with those obtained by experiment. This results indicate the validity of the predictive equation for the radial shrinkage by spot heating.

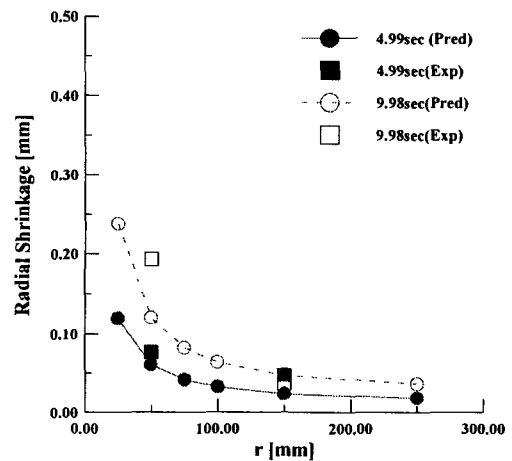


Fig. 13 Comparison results of radial shrinkage by spot heating with heating time



## 5. Conclusion

FEA and experimental studies have been performed with reference to torch tip number and heating variables to establish the proper spot heating conditions and the predictive equation for radial shrinkage. The main results obtained are summarized as follow.

1. The heat input models for flame torch tips (500, 800, 2000) were established by comparing the changes of temperature measured with that obtained by FEA.

2. Proper conditions for spot heating with air cooling condition were established by the extensive FEA.

3. For the spot heating condition established, the radial shrinkage increases linearly with an increase of the ratio of thermal energy to in-plane rigidity of the plate. In addition, the angular distortion could be controlled below  $2.5 \times 10^{-3}$  radian. Based on the these results, A predictive equation for radial shrinkage distribution at the spot heated plate was established by analytical solution and verified by comparing it with the results obtained by FEA and experiment.

## References

1. Y. Tomita, K. Hasimoto, N. Osawa, and N. Shinkai : Study on heat transfer between gas flame and steel plate during line heating process, *Proc. the 12th Asian Technical Exchange and Advisory Meeting on Marine Structure*, (1998), pp. 355-364
2. I. Tsuji, Y. Okumura : A Study on line heating process for plate bending of ship steels, *Journal of The West-Japan Society of Naval Architects*, Vol. 76, (1988), pp. 149-160